

Research Article: New Research / Development

## Caveolin1 identifies a specific subpopulation of cerebral cortex callosal projection neurons (CPN) including dual projecting cortical callosal/frontal projection neurons (CPN/FPN)

Jessica L. MacDonald<sup>1</sup>, R. M. Fame<sup>1</sup>, E. M. Gillis-Buck<sup>1</sup> and Jeffrey D. Macklis<sup>1</sup>

<sup>1</sup>Department of Stem Cell and Regenerative Biology, Center for Brain Science, and Harvard Stem Cell Institute, Harvard University, Cambridge, Massachusetts 02138, USA

DOI: 10.1523/ENEURO.0234-17.2017

Received: 5 July 2017

Revised: 11 December 2017

Accepted: 19 December 2017

Published: 8 January 2018

**Author Contributions:** JLM, RMF, and JDM designed research; JLM, RMF, and EGB performed experiments; JLM and RMF analyzed data; JLM, RMF, and JDM wrote the paper.

**Funding:** <http://doi.org/10.13039/100000065HHS> | NIH | National Institute of Neurological Disorders and Stroke (NINDS)  
R37 NS41590  
NS45523  
NS49553  
NS075672

**Funding:** Jane and Lee Seidman Fund

**Funding:** Emily and Robert Pearlstein Fund

**Funding:** United Sydney Association

**Funding:** <http://doi.org/10.13039/100000002HHS> | National Institutes of Health (NIH)  
F31 NS073163

**Conflict of Interest:** Authors report no conflict of interest.

This work was supported by grants from the N.I.H. (R37 NS41590, with additional infrastructure support by NS45523, NS49553, and NS075672), the Jane and Lee Seidman Fund, the Emily and Robert Pearlstein Fund, and the United Sydney Association (to J.D.M); National Science Foundation Graduate Research Fellowship Program (GRFP) fellowship, and National Institutes of Health predoctoral NRSA fellowship F31 NS073163 (to R.M.F).

J.L.M. and R.M.F. contributed equally to this work

**Correspondence should be addressed to:** Jeffrey D. Macklis, [jeffrey\\_macklis@harvard.edu](mailto:jeffrey_macklis@harvard.edu) or Jessica L. MacDonald: [jemacdon@syr.edu](mailto:jemacdon@syr.edu)

**Cite as:** eNeuro 2018; 10.1523/ENEURO.0234-17.2017

**Alerts:** Sign up at [eneuro.org/alerts](http://eneuro.org/alerts) to receive customized email alerts when the fully formatted version of this article is published.

Accepted manuscripts are peer-reviewed but have not been through the copyediting, formatting, or proofreading process.

Copyright © 2018 MacDonald et al.

This is an open-access article distributed under the terms of the Creative Commons Attribution 4.0 International license, which permits unrestricted use, distribution and reproduction in any medium provided that the original work is properly attributed.

- 1 **1. Title:** Caveolin1 identifies a specific subpopulation of cerebral cortex callosal projection  
2 neurons (CPN) including dual projecting cortical callosal/frontal projection neurons  
3 (CPN/FPN)
- 4 **2. Abbreviated Title:** Cav1 identifies dual-projecting CPN/FPN
- 5 **3. Authors:** MacDonald, JL\*<sup>§1,2</sup>; Fame, RM<sup>§1</sup>; Gillis-Buck, EM<sup>1</sup>; and Macklis, JD\*<sup>1</sup>  
6 <sup>§</sup> These authors contributed equally to this work  
7 \* Co-corresponding authors
- 8 **Author Affiliations:** <sup>1</sup>Department of Stem Cell and Regenerative Biology, Center for Brain  
9 Science, and Harvard Stem Cell Institute, Harvard University, Cambridge, Massachusetts,  
10 02138, <sup>2</sup>Current address: Department of Biology, Syracuse University, Syracuse, New York,  
11 13244.
- 12 **4. Author Contributions:** JLM, RMF, and JDM designed research; JLM, RMF, and EGB  
13 performed experiments; JLM and RMF analyzed data; JLM, RMF, and JDM wrote the paper.
- 14 **5. Correspondence should be addressed to:**  
15 Jeffrey D. Macklis: jeffrey\_macklis@harvard.edu or  
16 Jessica L. MacDonald: jemacdon@syr.edu
- 17 **6. Number of Figures:** 6 **7. Number of Tables:** 0
- 18 **8. Number of Multimedia:** 0 **9. Number of words in Abstract:** 234
- 19  
20 **10. Number of words in Significance Statement:** 113
- 21  
22 **11. Number of words in Introduction:** 905
- 23 **12. Number of words in Discussion:** 1422
- 24 **13. Acknowledgements:** We thank members of the Macklis lab for thoughtful discussions and  
25 input, in particular G. Cederquist for sharing expertise regarding CPN/BPN; and L. Pasquina,  
26 R. Richardson, C. Greppi, T. Keefe, and P. Davis for superb technical assistance.
- 27 **14. Conflict of Interest:** Authors report no conflict of interest.
- 28 **15. Funding Sources:** This work was supported by grants from the N.I.H. (R37 NS41590, with  
29 additional infrastructure support by NS45523, NS49553, and NS075672), the Jane and Lee  
30 Seidman Fund, the Emily and Robert Pearlstein Fund, and the United Sydney Association (to  
31 J.D.M); National Science Foundation Graduate Research Fellowship Program (GRFP)  
32 fellowship, and National Institutes of Health predoctoral NRSA fellowship F31 NS073163  
33 (to R.M.F).

35 **Abstract:**

36 The neocortex is composed of many distinct subtypes of neurons that must form precise  
37 subtype-specific connections to enable the cortex to perform complex functions. Callosal  
38 projection neurons (CPN) are the broad population of commissural neurons that connect the  
39 cerebral hemispheres via the corpus callosum. Currently, how the remarkable diversity of CPN  
40 subtypes and connectivity is specified, and how they differentiate to form highly precise and  
41 specific circuits, are largely unknown. We identify in mouse that the lipid-bound scaffolding  
42 domain protein Caveolin 1 (CAV1) is specifically expressed by a unique subpopulation of layer  
43 V CPN that maintain dual ipsilateral frontal projections to premotor cortex. CAV1 is expressed  
44 by over 80% of these dual projecting CPN/FPN (callosal/frontal projection neurons), with  
45 expression peaking early postnatally as axonal and dendritic targets are being reached and  
46 refined. CAV1 is localized to the soma and dendrites of CPN/FPN, a unique population of  
47 neurons that shares information both between hemispheres and with premotor cortex, suggesting  
48 function during post-mitotic development and refinement of these neurons, rather than in their  
49 specification. Consistent with this, we find that *Cav1* function is not necessary for the early  
50 specification of CPN/FPN, or for projecting to their dual axonal targets. CPN subtype-specific  
51 expression of *Cav1* identifies and characterizes a first molecular component that distinguishes  
52 this functionally unique projection neuron population, a population that expands in primates, and  
53 is prototypical of additional dual and higher-order projection neuron subtypes.

54

55

56

57 **Significance Statement:**

58 Callosal projections neurons (CPN) are a diverse set of neocortical interhemispheric  
59 excitatory projection neurons that integrate multiple distinct brain regions. While retrograde  
60 studies have identified CPN subpopulations that project to multiple targets, molecular identifiers  
61 are lacking for these subpopulations. Here, we identify *Caveolin1* (*Cav1*) as an identifier of CPN  
62 with dual callosal and ipsilateral frontal projections (CPN/FPN). CAV1 is expressed by over  
63 80% of these CPN/FPN, with expression peaking early postnatally. CAV1 localizes to the soma  
64 and dendrites of CPN/FPN, suggesting function during post-mitotic development and refinement  
65 of these neurons, rather than in their early specification. Identification of this molecular identifier  
66 of CPN/FPN will enable future functional investigations of this unique neuronal population.

67  
68 **Introduction:**

69 The neocortex is composed of many distinct subtypes of neurons that developmentally form  
70 precise subtype-specific connectivity and circuitry to enable cortex to perform its many complex  
71 functions of sensory processing, associative integration, cognition, and motor output. Callosal  
72 projection neurons (CPN) are the broad population of commissural neurons that connect the  
73 cerebral hemispheres via the corpus callosum (CC). CPN are excitatory pyramidal projection  
74 neurons whose cell bodies reside in neocortical layers II/III (~80% in mouse), V (~20%), and a  
75 few % in VI (Ivy and Killackey, 1981; Silver et al., 1982; Catapano et al., 2001; Fame et al.,  
76 2011; Greig et al., 2013; MacDonald, 2013), and play multiple roles in complex associative and  
77 integrative cognition. CPN are a diverse set of subpopulations, distinguished by characteristics  
78 including cell body location, birthdate, electrophysiological and neurochemical properties,

79 dendritic tree distribution, axonal target(s), and molecular expression (Aboitiz and Montiel,  
 80 2003; Mitchell and Macklis, 2005; Benavides-Piccione et al., 2006; Molyneaux et al., 2009;  
 81 Fame et al., 2011; Otsuka and Kawaguchi, 2011; Fame et al., 2016a). While these properties  
 82 describe and categorize CPN, they also determine the function(s) of diverse CPN subtypes.

83 Molecular controls that both define and regulate development of these distinct CPN subtypes  
 84 are just beginning to be elucidated. A combinatorially-expressed set of genes that both define  
 85 CPN as a broad population and distinguish novel subpopulations of CPN during development  
 86 has been identified (Molyneaux et al., 2009), and a few molecular controls have been  
 87 investigated functionally. For example, SATB2 regulates CPN identity throughout the neocortex;  
 88 in the absence of its function, CPN project axons subcortically rather than across the corpus  
 89 callosum, and they take on some molecular characteristics of corticofugal projection neurons  
 90 (Alcamo et al., 2008; Britanova et al., 2008). Other molecular controls regulate specific aspects  
 91 of CPN development, and/or distinct subpopulations. *Cux1* and *Cux2* regulate dendritic  
 92 complexity and synapse formation of layer II/III CPN (Cubelos et al., 2010), and *Cux1* regulates  
 93 activity-dependent interhemispheric connectivity of CPN (Rodriguez-Tornos et al., 2016).  
 94 CITED2 regulates generation of layer II/III CPN throughout the neocortex, as well as areal  
 95 identity and neuronal connectivity specifically of somatosensory CPN (Fame et al., 2016b).  
 96 CTIP1, on the other hand, regulates specification of deep layer CPN (Woodworth et al., 2016).

97 *Caveolin1* (*Cav1*) was identified in Molyneaux, et al. (2009) as a CPN subpopulation-  
 98 restricted gene during neocortical development, with a peak of expression at postnatal day 3  
 99 (P3). *Cav1* encodes a membrane-bound scaffolding protein necessary for a range of cellular  
 100 processes, including functions related to the unique lipid raft structures it forms, caveolae. *Cav1*  
 101 is highly expressed broadly in developing blood vessels and endothelial cells, and is required for

102 their proper development (Razani et al., 2001; Schubert et al., 2002), and for blood-brain barrier  
 103 permeability (Zhao et al., 2014). While caveolae are not thought to exist in neurons (Head and  
 104 Insel, 2007), *Cav1* knockout mice exhibit neurological abnormalities including limb clasping,  
 105 abnormal spinning, muscle weakness, reduced activity, and gait abnormalities (Trushina et al.,  
 106 2006).

107 As a lipid raft scaffolding molecule, CAV1 interacts with multiple binding partners, some of  
 108 which are particularly compelling as components of neuronal function. CAV1 binds directly to  
 109 the calmodulin-dependent scaffolding protein striatin (Gaillard et al., 2001), which acts as a  
 110 signaling platform in dendritic spine signal transduction (Benoist et al., 2006), and SNAP25,  
 111 which complexes to CAV1 presynaptically upon synaptic potentiation (Braun and Madison,  
 112 2000). CAV1 plays roles in neurotrophin response, and has the ability to interact with  
 113 synaptosome complexes (Bilderback et al., 1997; Bilderback et al., 1999; Head and Insel, 2007).  
 114 CAV1 is required for estrogen receptor  $\alpha$  (ER $\alpha$ ) activation of the metabotropic glutamate  
 115 receptor, mGluR1 $\alpha$ , in hippocampal neurons, potentially acting in long-term depression  
 116 (Takayasu et al., 2010). CAV1 provides a scaffold for both the ER $\alpha$  voltage-dependent anion  
 117 receptor and one of its interactors, the IGF-1 receptor (Maggi et al., 2002; Marin et al., 2009), a  
 118 known positive regulatory pathway for corticospinal projection neuron axonal outgrowth  
 119 (Ozdinler and Macklis, 2006).

120 *Cav1* has additionally been implicated in neuronal differentiation from progenitors (Li et al.,  
 121 2011), synaptic ribbons in photoreceptors (Kachi et al., 2001), and other neurotransmitter  
 122 receptor functions including muscarinic cholinergic receptors and NMDA receptor NR2B (Lai et  
 123 al., 2004). Further, CAV1 interacts with Rho-family GTPase RAC1, and this interaction has been

124 directly implicated in neurite outgrowth (Kang et al., 2006). These neuronal-specific processes  
125 might account for some of the neurological deficits in *Cav1* loss-of-function mice described  
126 above, and additionally motivate this study of *Cav1* in CPN.

127       Here, we further identify that *Cav1* is highly expressed during axonal and dendritic  
128 development in a laminarly- and regionally-restricted subset of dual projecting CPN that extend  
129 both homotopic axonal connections to mirror image locations in the contralateral hemisphere,  
130 and rostral connections to ipsilateral frontal areas, sending information from sensory or motor  
131 functional areas to higher hierarchical cortical areas (here, these dual-projecting neurons are  
132 referred to as callosal projection neurons/frontal projection neurons; CPN/FPN) (Mitchell and  
133 Macklis, 2005). The majority of these CPN/FPN are located in neocortical layer Va in both the  
134 primary somatosensory area (S1) and in a large expansion in caudo-lateral secondary  
135 somatosensory neocortex (S2) (Mitchell and Macklis, 2005). While CPN/FPN have been  
136 identified anatomically, no molecular controls over this population's unique connectivity or  
137 function have been identified, limiting understanding of the development and function of these  
138 specialized dual-projecting neurons. Our investigations of *Cav1* expression and function reported  
139 here identify and characterize a first molecular component that distinguishes and might control  
140 aspects of this functionally unique projection neuron population.

141

## 142 **Materials and Methods:**

### 143 ***Mouse Lines***

144       All animal procedures were performed in accordance with the [Author University] animal  
145 care committee's regulations. *Caveolin1* null mice on a congenic C57/B16 background (B6.Cg-

146 *Cav1<sup>tm1Mls</sup>/J*) were obtained from The Jackson Laboratory (Bar Harbor, Maine, USA), strain  
 147 number 007083 (RRID:IMSR\_JAX:007083). The original targeted null mutation was generated  
 148 by Michael Lisanti at The Albert Einstein College of Medicine. A 2.2 kb region of the gene  
 149 including exons 1 and 2 and a portion of the promoter region was replaced with a neomycin  
 150 resistance cassette via homologous recombination (Razani et al., 2001).

151 BTBR acallosal mice on a congenic background (BTBR *T<sup>+</sup> tf/J*) were obtained from The  
 152 Jackson Laboratory (Bar Harbor, Maine, USA), strain number 002282  
 153 (RRID:IMSR\_JAX:002282) (Wahlsten et al., 2003). LP/J mice have been shown to be an  
 154 appropriate callosal control population for BTBR mice. LP/J mice (LP/J) were obtained from the  
 155 Jackson Laboratory (Bar Harbor Maine, USA), strain number 000676  
 156 (RRID:IMSR\_JAX:000676).

157 C57/Bl6 wildtype mice were obtained from The Jackson Laboratory  
 158 (RRID:IMSR\_JAX:000664) (Bar Harbor, Maine, USA), and were used to breed with *Cav1* null  
 159 mice, and for birthdating and electroporation experiments. FEZF2 mutants were generated by  
 160 Hirata and et al. (Hirata et al., 2004) (GenBank accession number: AB042399).

#### 161 ***Immunocytochemistry***

162 Immunocytochemistry was performed as follows. Briefly, brains were fixed by transcardial  
 163 perfusion with PBS, followed by 4% paraformaldehyde, and postfixed overnight at 4°C in 4%  
 164 paraformaldehyde. Brains were sectioned at 50µm on a vibrating microtome (Leica). Sections  
 165 were blocked in 0.3% BSA (Sigma), 8% goat or donkey serum, and 0.3% Triton X-100 (Sigma)  
 166 for 1 hour at room temperature, before incubation in primary antibody. Secondary antibodies  
 167 were selected from the Alexa series.



168 Antigen retrieval methods were required to expose antigens for some of the primary  
169 antibodies, including CAV1. Sections were incubated in 0.1M citric acid (pH=6.0) for 10 min at  
170 95-98°C, and sections were rinsed in PBS prior to blocking. For thymidine analogues (IdU,  
171 CldU), HCl antigen retrieval was required. Tissue was rinsed quickly in ddH<sub>2</sub>O and incubated in  
172 2N HCl for 2 hours at room temperature, and sections were rinsed in PBS prior to blocking.

173 Primary antibodies and dilutions were used as follows: rabbit anti-Caveolin-1, 1:500 (Cell  
174 Signaling #3238; RRID:AB\_2072166); goat anti-LMO4, 1:200 (Santa Cruz Biotech SC- 11122;  
175 RRID:AB\_648429); rat anti-CTIP2 1:500 (Abcam ab18465; RRID:AB\_2064130), mouse anti-  
176 BrdU, 1:500 (Becton Dickinson #347580; clone B44; RRID:AB\_10015219) (detects IdU); rat  
177 anti-BrdU, 1:500 (Accurate #OBT- 0030; clone BU1/75; RRID:AB\_2313756) (detects CldU);  
178 rabbit anti-GFP, 1:500 (Molecular Probes; RRID:AB\_221569); mouse anti-SATB2, 1:500  
179 (Abcam ab51502; RRID:AB\_882455); goat anti-BHLHB5, 1:200 (Santa Cruz SC-6045;  
180 RRID:AB\_2065343); rabbit anti-5-HT, 1:1000 (Immunostar 20080; RRID:AB\_572263).

# 181 *In situ hybridization*

182 Nonradioactive colorimetric *in situ* hybridization was performed using probes labeled with  
183 digoxigenin (dig)-UTP generated by reverse transcription PCR. The probe sequence for *Cav1*  
184 was previously published (Molyneaux et al., 2009). Postnatal tissue was fixed overnight in 4%  
185 paraformaldehyde at 4° C. Fixed tissue was sectioned on a VT1000S vibrating microtome (Leica  
186 Microsystems) to a thickness of 50 µm. Embryonic tissue was flash frozen in 2-methyl butane,  
187 embedded in TBS, and cryosectioned on a CM3050S cryostat (Leica Microsystems) to a  
188 thickness of 14µm. Sense probes were used as negative controls in all experiments. Sections  
189 were mounted on Superfrost plus slides ® (Fisher Scientific) and postfixes in 4% PFA in PBS

190 for 10 min, rinsed in PBS for 3 min., permeabilized in 0.3% Triton X-100 (Sigma) followed by  
 191 RIPA cell lysis buffer [150 mM Sodium chloride, 1% Triton X-100, 1% deoxycholic acid sodium  
 192 salt, 0.1% sodium dodesil sulfate, 50 mM Tris-HCl, pH 7.5, 2mM EDTA], re-fixed in 4% PFA,  
 193 acetylated for 15 min in 0.1M triethanolamine/ 0.4% HCl/0.25% acetic anhydride (Sigma), and  
 194 then prehybridized in 65°C hybridization buffer [50% formamide, 5x SSC, 5x Denhardt's  
 195 [1µg/mL Ficoll 400, 1µg/mL Polyvinylpyrrolidone, 1µg/mL BSA] , 500µg/mL sheared salmon  
 196 sperm DNA, 250µg/mL Yeast RNA]. Slides were incubated overnight (14-20 hours) at 65°C in  
 197 2µg/17mL dig-labeled probe in hybridization buffer in a plastic mailer. Slides were then  
 198 subjected to stringency washes in 2x SSC/ 50% formamide/ 0.1% Tween-20 at 65°C for 2 hours.  
 199 Sections were then rinsed in MABT [0.9M maleic acid (Sigma), 0.1M NaCl (Sigma), 0.0005%  
 200 Tween 20 (Sigma), 0.175M NaOH (Sigma)] at RT, blocked in 10% goat serum in MABT, and  
 201 incubated overnight in goat alkaline phosphatase-conjugated anti-dig (1:1000, Roche) primary  
 202 antibody in block. The following day, the slides were rinsed with MABT, followed by a 30 min.  
 203 wash in alkaline phosphatase reaction buffer [100mM Tris pH 9.5, 50mM MgCl<sub>2</sub>, 100mM NaCl,  
 204 0.1% Tween-20]. The alkaline phosphatase reaction was developed with 0.25 mg/mL nitro-blue  
 205 tetrazolium (NBT) / 125µg/mL 5-bromo-4-chloro-3'-indolylphosphate (BCIP) in phosphatase  
 206 reaction buffer, changing to fresh solution every 1-4 hours at RT or every 6-9 hours at 4°C.  
 207 When the reaction was complete, tissue was rinsed in 0.1% Tween-20 in PBS, postfixed in 4%  
 208 PFA for 30 min.

## 209 ***Retrograde labeling of cortical projection neurons***

### 210 *Perinatal retrograde labeling of CPN, CSMN, CStrPN, and ACN*

211 Perinatal retrograde labeling of CPN, and CSMN was performed using a Vevo 770

212 ultrasound backscatter microscopy system (VisualSonics, Toronto, Canada). Briefly, P1 pups of  
 213 either sex were anesthetized by hypothermia, and corpus callosum, or pons, respectively, were  
 214 injected under ultrasound guidance using a pulled glass micropipette (tip diameter, 80–100  $\mu$ m),  
 215 and cell bodies were labeled with the  $\beta$  subunit of cholera toxin (CTB) labeled with Alexa dye (2  
 216 mg/ml, Molecular Probes). For CSMN, six 23 nl injections of cholera toxin subunit- B (2  $\mu$ g/ $\mu$ l)  
 217 were deposited bilaterally into the pons. The brains were harvested 2 days after injection (P3).

218 Because CStrPN reach the striatum later than P1, pups were anesthetized with  
 219 hypothermia and injected stereotactically at P3. The striatal injection point is very close to the  
 220 anterior commissure in the developing brain, so both CStrPN and ACN were labeled  
 221 simultaneously. The injections were made at an angle of 32.5° from horizontal, 3 mm posterior  
 222 to bregma, and 1.8mm lateral (left). The  $\beta$  subunit of cholera toxin (CTB) labeled with Alexa  
 223 dye (2 mg/ml, Molecular Probes) was injected at a depth of 4.2 mm, and 4.6 nL of dye was  
 224 delivered three times (total of 13.8 nL) into 3 injection sites at depths, 4.2 mm, 4.1 mm, and 4.0  
 225 mm. The needle was removed after 5 minutes to allow diffusion and avoid retracting the dye  
 226 with the needle. The brains were harvested 2 days after injection (P5).

#### 227 Postnatal dual CPN/FPN and CPN/BPN retrograde labeling

228 P6 pups were anesthetized with hypothermia. P21 mice were deeply anesthetized with  
 229 Avertin (0.02mL/g body weight, injected I.P.). Tracers were injected transcranially with sharp  
 230 pulled glass micropipettes (tip diameter 80-100 $\mu$ m) in presumptive premotor and sensory-motor  
 231 areas, as described below. Double fluorescent tracer injections were performed to label  
 232 simultaneously: 1) CPN in sensory-motor cortex, and 2) frontal projection neurons with long-  
 233 distance ipsilateral projections to the premotor cortex. CPN with projections to the contralateral

neocortex were labeled with Alexa 647 conjugated cholera toxin subunit  $\beta$  (2 mg/ml, Molecular Probes) with 25 injection sites, 46nL (10 injections of 4.6nL) each site at a depth of 250  $\mu$ m at P6 and 450 $\mu$ m at P21. The most caudal injection site was 1 mm caudal to bregma, and the most rostral injection-site was approximately 1 mm caudal to the olfactory bulbs. All other injections were evenly spaced to complete the 5 x 5 grid. Ipsilateral corticocortical projections to the premotor cortex were simultaneously retrogradely labeled with injections of Alexa 555 conjugated cholera toxin subunit B (2 mg/ml, Molecular Probes) with 7 injection sites, 46nL each site and a depth of 250 $\mu$ m at P6 and 450 $\mu$ m at P21 (see **Figure 4**). Brains were harvested 2 days after injection (P8).

Backward projecting neurons (BPN) were retrogradely labeled via transcranial injection of cholera toxin subunit B (2 mg/ml, Molecular Probes) at P7 into the ipsilateral caudal cortex, covering the area of the presumptive somatosensory cortex. The most rostralateral injection site was 1.5 mm rostral to lambda, and 2.5 mm lateral to the midline. All other injections were evenly spaced to complete the 3  $\times$  4 grid. Each mouse received ten 4.6 nl volume injections at 12 injection sites. For each injection site, 5 injections were made at 200  $\mu$ m depth from the dorsal surface of the brain, 2 injections at 150  $\mu$ m depth, 1 injection at 100  $\mu$ m depth, and 2 injections at 50  $\mu$ m depth. Brains were harvested 2 days after injection (P9).

Small punctures were made in the skull at the location of each injection point with either a pulled glass pipette (P6) or a fine suture needle (P21) prior to lowering the injection needle to the proper depth. This avoided the need for large craniotomies, thus minimizing insult and enhancing recovery time, while allowing for exact depth measurements to be made accurately.

255 For all retrograde labeling experiments, our approaches minimized surgical time and insult; thus  
256 morbidity was very low, and the survival rate was near 100%.

### 257 ***Birthdating***

258 For IdU and CldU birthdating, equimolar delivery of IdU (57.5 mg per kg) or CldU (42.5 mg  
259 per kg) was performed by intraperitoneal injections at 12 hour intervals from E11 to E15.5 (Vega  
260 and Peterson, 2005), calculating embryonic age with E0.5 as the morning of observed vaginal  
261 plug. Mice of either sex were perfused at P6, and brains prepared for immunocytochemistry.

### 262 ***Gain-of-function constructs***

263 For control gain-of-function experiments, a vector containing a constitutively active CMV  
264 enhancer /  $\beta$  actin promoter driving GFP downstream of an internal ribosomal entry site (IRES)  
265 was used (*GFP<sup>control</sup>*, generous gift of C. Lois, MIT; (Molyneaux et al., 2005)). For the *Cav1*  
266 overexpression construct, called *Cav1<sup>GFP</sup>*, full length *Cav1* cDNA was cloned into the same  
267 vector backbone using a Sal1/Not1 digest (New England Biolabs, Ipswich, MA) of the *Cav1*  
268 cDNA from a pSport1 vector purchased from Open Biosystems (Lafayette, CO; clone ID  
269 30062454 ). A sequenced clone with perfect alignment to the NCBI reference sequence  
270 NM\_007616 in both the sense and antisense orientations was selected for experiments.

### 271 ***In utero electroporation***

272 *In utero* electroporations were performed essentially as described in (Saito and Nakatsuji,  
273 2001; Saito, 2006), and (Molyneaux et al., 2005). Timed pregnant mice were deeply anesthetized  
274 with isofluorane. Hair was removed from the abdomen, and the dam was secured supine on a  
275 heated surgical platform. Individual pups were withdrawn from the abdominal cavity and  
276 moistened with sterile 37°C 1x PBS. Using a Vevo 770 ultrasound backscatter microscopy

277 system (VisualSonics, Toronto, Canada) to visualize the lateral ventricles, a beveled glass  
 278 micropipette (50  $\mu$ m width) was inserted into one lateral ventricle of each injected pup, and  
 279 fifteen 69 nl volume injections of prepared DNA mixture were delivered to the ventricle. Soon  
 280 after retracting the glass micropipette, electric current was applied to the head of the embryo  
 281 through two 1-cm diameter platinum electrodes, orienting the current to drive the negatively  
 282 charged DNA into the dorsal telencephalon. Five 25 volt pulses of 50 ms duration at 1 second  
 283 intervals were delivered using a CUY21EDIT square wave electroporator (Nepa Gene, Japan).  
 284 Each injected embryo was gently returned to the abdominal cavity, and the next selected embryo  
 285 was carefully withdrawn. No more than 6 embryos of either sex were injected per dam. The  
 286 abdomen was sutured. Dams recovered on a warm heating pad, and once ambulatory were  
 287 administered 250  $\mu$ l of buprenorphine (0.015 mg/ml sterile PBS) before returning to their cages.

#### 288 *Quantification of FPN/CPN*

289 For P8 quantification of Cav1-expressing CPN/FPN, anatomically matched sections were  
 290 selected ( $n = 4$  WT), and Cav1 immunocytochemistry was performed. Digital boxes of fixed  
 291 width indicated each of the four cortical regions, and the number of CPN/FPN and Cav1<sup>+</sup>  
 292 CPN/FPN were counted. Percentages of FPN/CPN that express Cav1 in each region were  
 293 calculated from total numbers. Error bars or “ $\pm$ ” indicate the standard error of the mean.  
 294 Individuated neuronal somata were counted for each assignment; it was not possible to count all  
 295 CPN or Cav1-expressing neurons in some densely packed microdomains due to high neuronal  
 296 density.

297 For P8 quantification of CPN/FPN in *Cav1*-null mice, anatomically matched sections were  
 298 selected ( $n = 6$  WT,  $n = 6$  *Cav1*<sup>-/-</sup>). Digital boxes of fixed width indicated the S1 or S2 cortical

regions, and the number of CPN/FPN, and FPN were counted in S1 and S2. The percent of FPN with concurrent callosal projections was also calculated. No significant differences were detected between WT and *Cav1<sup>-/-</sup>*. Error bars or “ $\pm$ ” indicate the standard error of the mean. Data were analyzed by unpaired Student’s t-test. Statistical analyses were performed in Prism (Graphpad Software, Inc.). A two-tailed post-hoc observed power was calculated from Cohen’s d, the p-value, and N.

	<i>Data Structure</i>	<i>Type of Test</i>	<i>N (WT; KO)</i>	<i>p-value</i>	<i>Observed Power</i>	<i>95% Confidence Interval</i>
<i>Figure 6G(S1)</i>	Gaussian	Unpaired t-test	(6; 6)	0.3585	0.4391	-9.642 - 24.31
<i>Figure 6G(S2)</i>	Gaussian	Unpaired t-test	(6; 6)	0.2831	0.4278	-21.05 - 64.72
<i>Figure 6H(S1)</i>	Gaussian	Unpaired t-test	(6; 6)	0.4056	0.4316	-111.2 - 253.2
<i>Figure 6H(S2)</i>	Gaussian	Unpaired t-test	(6; 6)	0.3004	0.4050	-18.72 - 54.72
<i>Figure 6I(S1)</i>	Gaussian	Unpaired t-test	(6; 6)	0.4529	0.4529	-0.3069 - 0.1476
<i>Figure 6I(S2)</i>	Gaussian	Unpaired t-test	(6; 6)	0.6214	0.6214	-0.1722 - 0.1081

### ***Microscopy and image analysis***

Whole mount images were acquired using an SMZ1000 fluorescence dissecting microscope (Nikon, Melville, NY) with a SPOT CCD digital camera (Diagnostic Instruments, Sterling Heights, MI) and SPOT acquisition software.

Tissue sections were imaged on a Nikon E1000 microscope (Nikon Instruments, Melville, NY) equipped with an XCite 120 illuminator (EXFO, Mississauga, ON, Canada) and Q-imaging Retixa EX cooled CCD camera (Q-imaging Corp., Surrey, BC, Canada), or a Nikon 90i microscope using a 1.5 megapixel cooled CCD digital camera (Andor Technology, Dublin, Northern Ireland), a 5 megapixel color CCD digital camera (Nikon Instruments, Melville, NY). Images were collected and analyzed with Volocity image analysis software (Version 4.0.1; Improvision Inc., Waltham, MA) or Elements acquisition software (Nikon Instruments, Melville,



317 NY).

318 Laser confocal analysis was performed using a BioRad Radiance 2100 confocal microscope  
319 with LaserSharp2000 imaging software (BioRad Laboratories, Hurcules, CA). Images were  
320 processed using a combination of functions provided by ImageJ (Rasband, W.S., ImageJ, U. S.  
321 National Institutes of Health, Bethesda, Maryland, USA, <http://imagej.nih.gov/ij/>, 1997-2011.)  
322 and Adobe Photoshop/ Illustrator software packages (Adobe, San Jose, CA).

323

## 324 **Results:**

### 325 *Cav1 is expressed by a restricted population of CPN, and is excluded from CSMN*

326 *Cav1* is highly expressed by CPN relative to corticospinal motor neurons (CSMN) in the  
327 developing neocortex, with a peak of expression between P3 and P6 (Molyneaux et al., 2009),  
328 during the critical time when CPN are making axonal and dendritic connections. *Cav1* is not  
329 detected in CPN by P14. We more thoroughly investigated CAV1 expression by  
330 immunocytochemistry, and similarly identified that CAV1 is indeed expressed by CPN in  
331 cortical layer Va, and is excluded from subcerebral projection neurons (SCPN, of which CSMN  
332 are a subpopulation) by combining CAV1 immunocytochemistry and dual retrograde labeling of  
333 CPN (from the contralateral cortex) and SCPN (from the pons) (**Figure 1A-C**). The CAV1-  
334 expressing population of CPN is clearly superficial to the SCPN (**Figure 1C**), and CAV1 is co-  
335 expressed with SATB2 (Figure 1D), which is expressed by CPN and excluded from SCPN.  
336 CAV1 expression is unchanged in *Fezf2* loss-of-function neocortex, in which no subcerebral  
337 neurons are specified (Molyneaux et al., 2005), confirming that CAV1 is excluded from CSMN  
338 (**Figure 1E-F**). The highly restricted expression pattern suggests that *Cav1* functions in a very



specific subpopulation of CPN, rather than playing a broad role in CPN development (**Figures 1, 2**).

Developmentally, Cav1 mRNA is not detected in pallial progenitors or the cortical plate at E13.5, but it is detected in the caudo-lateral cortical plate by E15.5 (**Figure 2A**). Both *Cav1* mRNA and CAV1 protein are detected in cortical neurons at E18.5 (in addition to developing blood vessels), are highly expressed at P3 and P6, and are no longer detectable by P14 (**Figure 2B, C**). *Cav1*-expressing neurons are distributed uniquely in cortical layer Va, especially in caudo-lateral areas. This pattern is not a developmental gradient, and is maintained specifically at all developmental ages at which *Cav1* is expressed (**Figure 2**).

Interestingly, CAV1 expression is restricted at P8 to a subpopulation of CPN extending in layer Va throughout primary somatosensory cortex (S1), and expanding in the caudo-lateral cortex (S2), and auditory cortex (A1) more caudally, but is mostly excluded from motor cortex (M1). This exclusion is clear by comparison between CAV1 immunocytochemistry and LMO4, which is highly expressed by CPN in motor cortex, but excluded from layer II/III CPN in somatosensory cortex (Azim et al., 2009; Huang et al., 2009) (**Figure 3A**). This area-specific expression further supports subpopulation-specific function of CAV1 in CPN. Because of the strong expression of CAV1 at all developmental ages in layer Va, particularly in caudo-lateral areas close to archicortex, where canonical cortical neuron subpopulations are not maintained, we investigated whether CAV1-expressing neurons exclude CTIP2, the canonical postmitotic SCPN control transcription factor highly expressed by specific SCPN layer V populations (Arlotta et al., 2005; Chen et al., 2008). There is very little overlap between CAV1 and CTIP2 in S1 (**Figure 3B**), though a small subset of CAV1-expressing neurons in far caudo-lateral S2 express CTIP2 (**Figure 3C**). Based on size and morphology, these CAV1+/CTIP2+ neurons

362 appear to be pyramidal projection neurons; however, they do not appear to project subcerebrally,  
 363 as determined by the lack of overlap between CAV1 and retrogradely-labeled SCPN (Figure 1).  
 364 This quite unique population of non-SCPN, CTIP2<sup>+</sup> neurons has not been extensively defined,  
 365 but they might be a subpopulation of neurons with a transient developmental spinal projection  
 366 that is later lost (Polleux et al., 2001; Arlotta et al., 2005).

367 To investigate more deeply what subpopulation(s) of CPN express CAV1, we examined  
 368 expression of CAV1 in comparison to lamina-restricted molecular markers (Figure 3D). CAV1 is  
 369 co-expressed with Bhlhb5, which is expressed in layers II-V, while CAV1 is expressed below the  
 370 layer IV barrel field, as indicated by 5-HT expression. Thus, CAV1 is expressed in layer V.  
 371 Further, to better delineate the population(s) and to enable optimal targeting of the population via  
 372 *in utero* electroporation in future experiments, we performed birthdating analysis with thymidine  
 373 analogs every 12 hours throughout corticogenesis. These experiments reveal that CAV1-  
 374 expressing neurons are born between E12.5 and E13.5, consistent with the dominant birthdate  
 375 ranges for neocortical neurons residing in layer V (**Figure 3E**). CAV1-expressing neurons in  
 376 caudo-lateral S2 cortex might be born a few hours earlier (peak at E12.5) than those of S1 layer  
 377 V (peak at E13.5).

### 378 ***CAV1 is expressed by over 80% of dual-projecting FPN/CPN***

379 Development of CPN does not end when early progenitors are specified, but, rather, includes  
 380 acquisition of specific CPN subpopulation identities. Beyond the fact that CAV1 is highly  
 381 expressed by CPN compared to CSMN overall, it is further quite specifically expressed in a very  
 382 restricted pattern in neocortex. Because many uniquely projecting subpopulations of CPN reside  
 383 in restricted cortical areas (in particular, within layer V) (Fame et al., 2011), and because the  
 384 location of maximal CAV1 expression was reminiscent of the location of dual projecting neurons

385 in mouse neocortex (Mitchell and Macklis, 2005), we investigated potential CAV1 expression by  
 386 forward projecting neurons from somatosensory cortex to frontal areas (FPN), backward  
 387 projecting neurons (BPN), CPN with contralateral striatal projections (CStrPN<sub>i</sub>), and  
 388 commissural neurons with anterior commissure projections (ACN) (**Figure 4A-D**). The pattern  
 389 of CAV1 expression closely resembles the restricted location of dual projecting frontal/callosal  
 390 projection neurons (FPN/CPN) (Mitchell and Macklis, 2005), and partially overlaps with the  
 391 location of CStrPN<sub>i</sub> and ACN in the most lateral regions. Expression is highest at the time of  
 392 axon and dendrite extension, and formation and stabilization of neuronal connections (P3)  
 393 (**Figure 2**). The rostral location of BPN does not overlap with the CAV1 expression domain,  
 394 indicating that CAV1 is not expressed by all dual projecting CPN populations; CAV1 expression  
 395 is quite specific. Although some CStrPN<sub>i</sub>/ACN are located within the CAV1 expression domain  
 396 laterally, the location of FPN/CPN closely overlaps with the CAV1 expression domain,  
 397 suggesting that CAV1 might be specifically important for CPN/FPN development, connectivity,  
 398 and/or function (**Figure 4**).

399 To confirm more deeply at the individual neuron level whether CAV1 is expressed by the  
 400 dual projecting FPN/CPN subpopulation, we retrogradely co-labeled callosal- and frontal-  
 401 projecting neurons by stereotaxic injection of the beta subunit of cholera toxin conjugated to two  
 402 different Alexa fluorophores into the contralateral somatosensory cortex and the ipsilateral  
 403 premotor cortex, respectively (**Figure 4E-F**). CAV1 overlaps with the entire domain of FPN,  
 404 which also exist in other sensory modalities, including A1 (Mitchell and Macklis, 2005). We  
 405 verified the proportion of CPN/FPN that express CAV1 in S1 and S2, since they represent the  
 406 major population of CPN/FPN. We found that over 80% of dual projecting CPN/FPN are  
 407 CAV1<sup>+</sup>, and only a small population of non-dual projecting cortical neurons expresses CAV1;

408 CAV1 expression is thus highly restricted to and quite specific for this dual projecting population  
 409 (**Figure 4F**). Though the membranous location of CAV1 protein and the incomplete label  
 410 generated by CTB injections preclude equivalent and reciprocal quantification of the percentage  
 411 of CAV1<sup>+</sup> cortical neurons that are dual-projecting, the domains map closely to the single neuron  
 412 level.

413 *CAV1 is localized to CPN cell bodies and dendrites, and expression is not dependent on*  
 414 *correct callosal connectivity*

415 CAV1 is a membrane-bound scaffolding protein, so its subcellular distribution might provide  
 416 insight into its function(s) in specific neuronal subtypes. We investigated the subcellular  
 417 localization of CAV1 in P3 CPN, and found it to be highly localized around the soma, extending  
 418 throughout the apical dendrite and dendritic tuft (**Figure 5A**). The same subcellular localization  
 419 is observed at later stages of development (P7, data not shown). CAV1 is not highly detected in  
 420 axons. This suggests potential roles for CAV1 in migration and/or dendrite function, though  
 421 function at lower concentration in axons or growth cones is not excluded. Further, we generated  
 422 a *Cav1-IRES-GFP* over-expression construct, and exogenously over-expressed *Cav1* in layer  
 423 II/III CPN of somatosensory cortex via *in utero* electroporation at E15.5. Superficial layer CPN,  
 424 which do not normally express *Cav1*, show a similar cellular distribution of CAV1 to that of  
 425 endogenous neurons, with strong localization around CPN somata and in apical dendrites at P6  
 426 (**Figure 5B**). This is in direct contrast to over-expressed GFP, which is evenly distributed  
 427 throughout the neuronal soma, dendritic arbor, and axons, in which it is readily detectable  
 428 (**Figure 5C, B''**).

429 Since CAV1 is known to interact with striatins for correct signal transduction at synapses  
 430 (Gaillard et al., 2001), and with multiple neurotransmitter receptors (Boulware et al., 2007;

431 Takayasu et al., 2010), we considered that CAV1 expression might be regulated by neuronal  
 432 activity. However, based on the early neonatal expression of CAV1, we hypothesized that final  
 433 connectivity is not needed for CAV1 expression. To investigate whether CPN connectivity is  
 434 required for postnatal CAV1 expression, we investigated whether CAV1 expression is altered in  
 435 acallosal BTBR mice (Wahlsten et al., 2003). The BTBR mouse strain exhibits otherwise largely  
 436 normal cortical development, but no axons extend across the CC. Even though they perform  
 437 quite well on physical coordination tasks, they display behavioral abnormalities. Additionally,  
 438 these mice exhibit a reduced hippocampal commissure, accompanied by improper wiring  
 439 reflected by tangles of axons known as probst bundles. These experiments reveal that CAV1  
 440 expression is independent of correct callosal connectivity, and CAV1 is expressed normally in  
 441 P4 BTBR neocortex (**Figure 5D**). Taken together, these results indicate that, although CAV1 had  
 442 been previously shown to act at synapses (Gaillard et al., 2001), its expression by developing  
 443 CPN is not dependent on correct connectivity.

444 ***Cav1 function is not necessary for dual-projecting FPN/CPN to reach their axonal targets***

445 Because CAV1 is expressed by the overwhelming majority of dual-projecting FPN/CPN at  
 446 P8, and most highly at P3, and even though it not enriched in axons, we investigated whether  
 447 *Cav1* might be necessary for the correct maturation and/or maintenance of this specific  
 448 subpopulation of CPN. However, because of its subcellular localization to the somato-dendritic  
 449 compartments, we hypothesized that CAV1 would not be necessary for axonal guidance or  
 450 targeting. We first investigated whether axons of FPN/CPN initially reach their targets correctly  
 451 in the absence of *Cav1* function, which would indicate that *Cav1* is not necessary for axonal  
 452 extension, pathfinding, or establishment of CPN connectivity. We retrogradely labeled FPN/CPN  
 453 in both *Cav1* null mice and their wildtype (WT) littermates at P6, as described previously, and

454 examined them at P8 (Figure 6). At this relatively early time (P8), when CPN exuberance is most  
455 pronounced, there is no difference in the overall number of FPN/CPN between *Cav1* null and  
456 WT mice (Figure 6G), including within the secondary somatosensory cortical area (S2), where  
457 both CAV1 expression and the abundance of FPN/CPN change dramatically. Thus, as predicted  
458 by its subcellular localization, *Cav1* function is not required for CPN/FPN to extend dual-  
459 projecting axons to specific targets. Since CAV1 is localized around neuronal cell bodies and  
460 dendritic trees, but not substantially in axons, it is not surprising that FPN/CPN reach their  
461 targets at P8, further supporting somato-dendritic-specific function for *Cav1*.

462 CAV1 expression and localization in CPN/FPN during early neuronal maturation suggests  
463 subtype-specific function(s) during processes such as migration, neurite outgrowth, and  
464 branching. The previously known scaffolding roles of CAV1 at synapses, and its interactions  
465 with neurotransmitter receptors and Rac1 in other systems, suggest that CAV1 might influence  
466 neuronal activity through axonal/dendritic connectivity and/or function. Our results identify  
467 highly specific neocortical CAV1 expression in the dendritic compartment of dual projecting  
468 CPN/FPN, and further identifies both that CAV1 expression is not dependent on axonal  
469 connectivity, and that correct axonal targeting of CPN/FPN is independent of CAV1.

470

#### 471 **Discussion:**

472 Identifying molecular markers and determinants of distinct subsets of callosal projection  
473 neurons (CPN) of the cerebral cortex will enable specific and rigorous investigation of distinct  
474 and unique subpopulations potentially critical for information integration and associative  
475 connectivity. CPN reside in cortical layers II/III, V, and VI, and all extend axons to homotopic

476 targets in the contralateral hemisphere. Some CPN subpopulations extend second (or more)  
477 axons to distinct targets including frontal or caudal ipsilateral neocortex, or even subcortically  
478 into ipsi- or contralateral striatum (Mitchell and Macklis, 2005; Cederquist et al., 2013; Sohur et  
479 al., 2014). Increasingly specific markers and determinants will also potentially enable in-depth  
480 functional analysis of these determinants themselves through development, to gain insight into  
481 their roles in establishing precise connectivity that endows specific CPN subpopulations with  
482 critical roles in neocortical information transfer, correlation, and integration.

483       Here, we identify that CAV1, a lipid raft scaffolding protein enriched in CPN over CSMN  
484 (Molyneaux et al., 2009), is expressed in a restricted fashion in the developing neocortex, and is  
485 expressed by over 80% of a unique, interesting, and likely functionally special CPN  
486 subpopulation – dual projecting CPN extending axons both contralaterally and to ipsilateral  
487 frontal areas (CPN/FPN). Comparative microarray analyses have identified molecular markers  
488 and determinants of CPN subpopulations, and subsequent evaluation of these and other data  
489 reveal molecular diversity within the broad population of CPN (Molyneaux et al., 2009; Fame et  
490 al., 2016a; Fame et al., 2016b). This diversity includes not only laminar and areal  
491 subpopulations, but also unique expression patterns that reflect subpopulations of CPN with  
492 distinct and sometimes multi-target axonal projections. CAV1 is a first studied example of such  
493 multi-target CPN identifiers; interestingly, it is localized to CPN cell bodies and dendrites, but is  
494 not detected in axons. The developmental temporal expression of *Cav1* coincides with the  
495 intermediate time period of CPN development, including low-level expression during neuronal  
496 migration, and highest levels of expression from P3 to P6 in mice, when CPN are extending and  
497 refining axonal and dendritic processes. Together, these results suggest functions for *Cav1* in  
498 post-mitotic establishment of innervation and/or pruning of connections.



499 CAV1 has a unique, areally-restricted expression pattern within CPN of layer Va; it is co-  
 500 expressed with BHLHB5 in S1, but excluded from the LMO4-expressing M1. The reciprocal  
 501 expression of LMO4 and BHLHB5 in M1 and S1, respectfully, is important for establishing  
 502 these areal identities (Joshi et al., 2008b; Cederquist et al., 2013). Further, *Lmo4* loss-of-function  
 503 disrupts the development of dual-projecting CPN/BPN, whose cell bodies reside in the rostral  
 504 motor cortex, and which send axons callosally and caudally (Cederquist et al., 2013). Thus, it is  
 505 interesting to speculate that *Bhlhb5* loss-of-function might similarly disrupt development of the  
 506 CAV1+ dual projecting CPN/FPN.

507 Here, we further report that *Cav1* function is not necessary for specification and early  
 508 development of dual projecting CPN/FPN, investigated by precise dual retrograde labeling  
 509 approaches in *Cav1* null neocortex. These results are consistent with Cav1's later developmental  
 510 timing of expression, and absence of subcellular localization to axons. Because these CPN/FPN  
 511 projections continue to prune and establish precise connectivity until P21 (Mitchell and Macklis,  
 512 2005), future studies might employ the same or related dual labeling approaches progressively to  
 513 or beyond P21 to investigate potential changes in axonal pruning that might result from  
 514 potentially improper dendritic arborization, dendritic synaptogenesis, and/or axonal target-  
 515 finding. If there is a change in the number of CPN/FPN in *Cav1* null mice at P21, comparison  
 516 between the number of CPN/FPN detected with retrograde labeling at P21 to the number  
 517 detected at P21 from retrograde labeling performed at P8, for example, would be able to  
 518 distinguish between axonal pruning of one or both projections, versus loss of these neurons  
 519 altogether.

520 Because of CAV1's known interaction with neurotransmitter receptors (Lai et al., 2004;  
 521 Boulware et al., 2007; Takayasu et al., 2010), dendritic spine signaling scaffolds (Gaillard et al.,



2001), and synaptosome components (Bilderback et al., 1997; Bilderback et al., 1999; Braun and Madison, 2000) function(s) of CAV1 in CPN/FPN might only be elucidated optimally through electrophysiological functional analysis of these neurons lacking their endogenous *Cav1* function in *in vivo* circuits. We find that *Cav1* expression is not dependent on correct CPN connectivity, by investigating CAV1 expression in the acallosal BTBR and *Fezf2*<sup>-/-</sup> mouse lines. However, *Cav1* might still be critical for CPN/FPN neuronal activity, since neuronal activity is often tightly tied to axonal and dendritic connectivity (Wang et al., 2007; Cubelos et al., 2010; Rodriguez-Tornos et al., 2016), especially establishment and maintenance. Studies examining P21 CPN/FPN axonal and dendritic morphologies with loss- or gain-of-function of *Cav1* might reveal CAV1 function(s) in CPN/FPN activity.

We also identify that CAV1 is highly concentrated in cell bodies and apical dendrites of CPN/FPN. Interestingly, CAV1 is also localized to the cell bodies and dendrites of a subpopulation of pyramidal cortical neurons in primates (Fame et al., 2016a), even though older studies suggest that CPN/FPN might not be maintained in primates, but, rather, might be pruned (Schwartz and Goldman-Rakic, 1982, 1984; Andersen et al., 1985; Johnson et al., 1989; Meissirel et al., 1991). Regardless of whether there are large or relatively rare primate CPN/FPN subpopulations, some unique properties of this subpopulation are likely conserved between mice and primates. Because of the identified conserved and specific subcellular localization of CAV1, future work might examine dendritic development and maintenance in *Cav1* null CPN/FPN in comparison to wildtype. Together, these studies could provide important insight into the development of this unique dual projecting population of CPN that likely function in a variety of complex and critical processes, integrating cortical information between hemispheres and from primary sensorimotor areas to premotor cortices.

545 Future studies could investigate whether CAV1 directly interacts in CPN with a subset of  
 546 previously identified CAV1 binding partners (particularly those shown to act in neuronal-  
 547 relevant processes), and whether CAV1 functions in the development of defined subpopulations  
 548 of CPN through these interactions. CAV1 is known to have a number of protein interactors from  
 549 studies in other systems. One particularly compelling potential interacting protein for first  
 550 analysis in CPN/FPN is Rac1, given that it has been shown in other systems to play roles in  
 551 important neuronal functions relating to cytoskeletal dynamics and focal adhesion, such as  
 552 neurite growth, adhesion, and migration (Beardsley et al., 2005; Kang et al., 2006; Joshi et al.,  
 553 2008a). In particular, Rac1 is required for midline crossing of CPN (Chen et al., 2007; Kassai et  
 554 al., 2008), and Rac1, recruited by CDKL5, can regulate neuronal migration and dendritic  
 555 arborization of some CPN (Chen et al., 2010). Identification of neocortical binding partners of  
 556 CAV1 could provide valuable insight into mechanisms of CPN subtype development /  
 557 refinement through complex networks of discrete protein-protein interactions, with potential  
 558 implications for subtypes of autism spectrum disorders (ASD) and/or schizophrenia. The  
 559 emerging “cortical connectivity/ synaptogenic hypothesis” of ASD suggests that such change(s)  
 560 caused by *Cav1* dysfunction might contribute to ASD and related behavioral phenotypes.

561 Interestingly, human *Cav1* is located at 7q31.1, part of autism-linked locus 9 (Auts9),  
 562 immediately upstream of *MET*, which shows direct pre-transcription start-site mutations  
 563 associated with ASD (Campbell et al., 2006). It might be that *Cav1* is also directly relevant in  
 564 ASD, and might potentially contribute to some of the Auts9 linkage to the disorders, perhaps via  
 565 CPN. *Cav1* is also close genomically to *Foxp2* in Auts9, which was initially suspected by some  
 566 to underlie ASD language defects, but was later shown to not be causal of the Auts9 ASD  
 567 linkage (Newbury et al., 2002). Other potential gene linkages in this locus (NRCAM and ST7)

568 are relatively weak, indicating that the linkage must be accounted for, at least in part, by other  
569 *Auts9* genes, potentially partially by *Cav1*. CAV1 has also been implicated as a potential target  
570 for schizophrenia therapy due to its interaction with DISC1, and its ability to modulate DISC1  
571 expression in neurons (Kassan et al., 2017).

572 The data we present here are, to our knowledge, the first identification of a potential  
573 molecular control over a unique and specialized dual projecting subpopulation of CPN,  
574 CPN/FPN. While CAV1 might likely function as a specific developmental and/or functional  
575 regulator in CPN/FPN, its specificity within this population also immediately provides a  
576 molecular marker. This will allow future studies to identify, genetically target, and/or purify this  
577 population to investigate and potentially discover additional potential upstream controls over  
578 CPN/FPN development. The defining properties of this CPN/FPN subpopulation, likely critical  
579 for “feed forward” information integration, are yet to be well understood, but analysis of *Cav1*  
580 expression and function identifies and characterizes a first molecular marker and determinant of  
581 this unique associative and integrative neocortical projection neuron population.

582

583

584 **References:**

585 Aboitiz F, Montiel J (2003) One hundred million years of interhemispheric communication: the  
586 history of the corpus callosum. *Braz J Med Biol Res* 36:409-420.

- 587 Alcamo EA, Chirivella L, Dautzenberg M, Dobрева G, Farinas I, Grosschedl R, McConnell SK  
588 (2008) Satb2 regulates callosal projection neuron identity in the developing cerebral  
589 cortex. *Neuron* 57:364-377.
- 590 Andersen RA, Asanuma C, Cowan WM (1985) Callosal and prefrontal associational projecting  
591 cell populations in area 7A of the macaque monkey: a study using retrogradely  
592 transported fluorescent dyes. *J Comp Neurol* 232:443-455.
- 593 Arlotta P, Molyneaux BJ, Chen J, Inoue J, Kominami R, Macklis JD (2005) Neuronal subtype-  
594 specific genes that control corticospinal motor neuron development in vivo. *Neuron*  
595 45:207-221.
- 596 Azim E, Shnyder SJ, Cederquist GY, Sohur US, Macklis JD (2009) Lmo4 and Clim1  
597 progressively delineate cortical projection neuron subtypes during development. *Cereb*  
598 *Cortex* 19 Suppl 1:i62-69.
- 599 Beardsley A, Fang K, Mertz H, Castranova V, Friend S, Liu J (2005) Loss of caveolin-1 polarity  
600 impedes endothelial cell polarization and directional movement. *J Biol Chem* 280:3541-  
601 3547.
- 602 Benavides-Piccione R, Hamzei-Sichani F, Ballesteros-Yanez I, DeFelipe J, Yuste R (2006)  
603 Dendritic size of pyramidal neurons differs among mouse cortical regions. *Cereb Cortex*  
604 16:990-1001.
- 605 Benoist M, Gaillard S, Castets F (2006) The striatin family: A new signaling platform in  
606 dendritic spines. *Journal of Physiology-Paris*.
- 607 Bilderback TR, Grigsby RJ, Dobrowsky RT (1997) Association of p75(NTR) with caveolin and  
608 localization of neurotrophin-induced sphingomyelin hydrolysis to caveolae. *J Biol Chem*  
609 272:10922-10927.

- 610 Bilderback TR, Gazula VR, Lisanti MP, Dobrowsky RT (1999) Caveolin interacts with Trk A  
 611 and p75(NTR) and regulates neurotrophin signaling pathways. *J Biol Chem* 274:257-263.
- 612 Boulware MI, Kordasiewicz H, Mermelstein PG (2007) Caveolin proteins are essential for  
 613 distinct effects of membrane estrogen receptors in neurons. *J Neurosci* 27:9941-9950.
- 614 Braun JE, Madison DV (2000) A novel SNAP25-caveolin complex correlates with the onset of  
 615 persistent synaptic potentiation. *J Neurosci* 20:5997-6006.
- 616 Britanova O, de Juan Romero C, Cheung A, Kwan KY, Schwark M, Gyorgy A, Vogel T,  
 617 Akopov S, Mitkovski M, Agoston D, Sestan N, Molnar Z, Tarabykin V (2008) *Satb2* is a  
 618 postmitotic determinant for upper-layer neuron specification in the neocortex. *Neuron*  
 619 57:378-392.
- 620 Campbell DB, Sutcliffe JS, Ebert PJ, Militerni R, Bravaccio C, Trillo S, Elia M, Schneider C,  
 621 Melmed R, Sacco R, Persico AM, Levitt P (2006) A genetic variant that disrupts *MET*  
 622 transcription is associated with autism. *Proc Natl Acad Sci USA* 103:16834-16839.
- 623 Catapano LA, Arnold MW, Perez FA, Macklis JD (2001) Specific neurotrophic factors support  
 624 the survival of cortical projection neurons at distinct stages of development. *J Neurosci*  
 625 21:8863-8872.
- 626 Cederquist GY, Azim E, Shnider SJ, Padmanabhan H, Macklis JD (2013) *Lmo4* establishes  
 627 rostral motor cortex projection neuron subtype diversity. *J Neurosci* 33:6321-6332.
- 628 Chen B, Wang SS, Hattox AM, Rayburn H, Nelson SB, McConnell SK (2008) The *Fezf2-Ctip2*  
 629 genetic pathway regulates the fate choice of subcortical projection neurons in the  
 630 developing cerebral cortex. *Proc Natl Acad Sci U S A* 105:11382-11387.

- 631 Chen L, Liao G, Waclaw RR, Burns KA, Linquist D, Campbell K, Zheng Y, Kuan CY (2007)
- 632 Rac1 controls the formation of midline commissures and the competency of tangential
- 633 migration in ventral telencephalic neurons. *J Neurosci* 27:3884-3893.
- 634 Chen Q, Zhu YC, Yu J, Miao S, Zheng J, Xu L, Zhou Y, Li D, Zhang C, Tao J, Xiong ZQ (2010)
- 635 CDKL5, a protein associated with rett syndrome, regulates neuronal morphogenesis via
- 636 Rac1 signaling. *J Neurosci* 30:12777-12786.
- 637 Cubelos B, Sebastian-Serrano A, Beccari L, Calcagnotto ME, Cisneros E, Kim S, Dopazo A,
- 638 Alvarez-Dolado M, Redondo JM, Bovolenta P, Walsh CA, Nieto M (2010) Cux1 and
- 639 Cux2 regulate dendritic branching, spine morphology, and synapses of the upper layer
- 640 neurons of the cortex. *Neuron* 66:523-535.
- 641 Fame RM, MacDonald JL, Macklis JD (2011) Development, specification, and diversity of
- 642 callosal projection neurons. *Trends Neurosci* 34:41-50.
- 643 Fame RM, Dehay C, Kennedy H, Macklis JD (2016a) Subtype-Specific Genes that Characterize
- 644 Subpopulations of Callosal Projection Neurons in Mouse Identify Molecularly
- 645 Homologous Populations in Macaque Cortex. *Cereb Cortex*.
- 646 Fame RM, MacDonald JL, Dunwoodie SL, Takahashi E, Macklis JD (2016b) Cited2 Regulates
- 647 Neocortical Layer II/III Generation and Somatosensory Callosal Projection Neuron
- 648 Development and Connectivity. *J Neurosci* 36:6403-6419.
- 649 Gaillard S, Bartoli M, Castets F, Monaghan AP (2001) Striatin, a calmodulin-dependent
- 650 scaffolding protein, directly binds caveolin-1. *FEBS Letters*.
- 651 Greig LC, Woodworth MB, Galazo MJ, Padmanabhan H, Macklis JD (2013) Molecular logic of
- 652 neocortical projection neuron specification, development and diversity. *Nat Rev Neurosci*
- 653 14:755-769.

- 654 Head BP, Insel PA (2007) Do caveolins regulate cells by actions outside of caveolae? Trends  
655 Cell Biol 17:51-57.
- 656 Hirata T, Suda Y, Nakao K, Narimatsu M, Hirano T, Hibi M (2004) Zinc finger gene fez-like  
657 functions in the formation of subplate neurons and thalamocortical axons. Dev Dyn  
658 230:546-556.
- 659 Huang Z, Kawase-Koga Y, Zhang S, Visvader J, Toth M, Walsh CA, Sun T (2009) Transcription  
660 factor Lmo4 defines the shape of functional areas in developing cortices and regulates  
661 sensorimotor control. Dev Biol 327:132-142.
- 662 Ivy GO, Killackey HP (1981) The ontogeny of the distribution of callosal projection neurons in  
663 the rat parietal cortex. J Comp Neurol 195:367-389.
- 664 Johnson PB, Angelucci A, Ziparo RM, Minciacchi D, Bentivoglio M, Caminiti R (1989)  
665 Segregation and overlap of callosal and association neurons in frontal and parietal  
666 cortices of primates: a spectral and coherency analysis. J Neurosci 9:2313-2326.
- 667 Joshi B, Strugnell SS, Goetz JG, Kojic LD, Cox ME, Griffith OL, Chan SK, Jones SJ, Leung SP,  
668 Masoudi H, Leung S, Wiseman SM, Nabi IR (2008a) Phosphorylated caveolin-1  
669 regulates Rho/ROCK-dependent focal adhesion dynamics and tumor cell migration and  
670 invasion. Cancer Res 68:8210-8220.
- 671 Joshi PS, Molyneaux BJ, Feng L, Xie X, Macklis JD, Gan L (2008b) Bhlhb5 regulates the  
672 postmitotic acquisition of area identities in layers II-V of the developing neocortex.  
673 Neuron 60:258-272.
- 674 Kachi S, Yamazaki A, Usukura J (2001) Localization of caveolin-1 in photoreceptor synaptic  
675 ribbons. Invest Ophthalmol Vis Sci 42:850-852.

- 676 Kang MJ, Seo JS, Park WY (2006) Caveolin-1 inhibits neurite growth by blocking Rac1/Cdc42  
677 and p21-activated kinase 1 interactions. *Neuroreport* 17:823-827.
- 678 Kassai H, Terashima T, Fukaya M, Nakao K, Sakahara M, Watanabe M, Aiba A (2008) Rac1 in  
679 cortical projection neurons is selectively required for midline crossing of commissural  
680 axonal formation. *European Journal of Neuroscience* 28:257-267.
- 681 Kassan A, Egawa J, Zhang Z, Almenar-Queralt A, Nguyen QM, Lajevardi Y, Kim K, Posadas E,  
682 Jeste DV, Roth DM, Patel PM, Patel HH, Head BP (2017) Caveolin-1 regulation of  
683 disrupted-in-schizophrenia-1 as a potential therapeutic target for schizophrenia. *J*  
684 *Neurophysiol* 117:436-444.
- 685 Lai H, Boone T, Yang G, Smith C, Kiss S, al. e (2004) Loss of caveolin-1 expression is  
686 associated with disruption of muscarinic cholinergic activities in .... *Neurochemistry*  
687 *International*.
- 688 Li Y, Luo J, Lau WM, Zheng G, Fu S, Wang TT, Zeng HP, So KF, Chung SK, Tong Y, Liu K,  
689 Shen J (2011) Caveolin-1 plays a crucial role in inhibiting neuronal differentiation of  
690 neural stem/progenitor cells via VEGF signaling-dependent pathway. *PLoS One*  
691 6:e22901.
- 692 MacDonald JL, Fame, R.M., Azim, E., Shnider, S.J., Molyneaux, B.J., Arlotta, P., and Macklis,  
693 J.D. (2013) Specification of Cortical Projection Neurons: Transcriptional Mechanisms.  
694 In: *Comprehensive Developmental Neuroscience: Patterning and Cell Type Specification*  
695 *in the Developing CNS and PNS* (Rubenstein JLaR, P, ed), pp 475-502: Elsevier.
- 696 Maggi D, Biedi C, Segat D, Barbero D, Panetta D, al. e (2002) IGF-I induces caveolin 1 tyrosine  
697 phosphorylation and translocation in the lipid rafts. *Biochemical and Biophysical*  
698 *Research Communications*.



- 699 Marin R, Díaz M, Alonso R, Sanz A, Arévalo MA, Garcia-Segura LM (2009) Role of estrogen  
700 receptor  $\alpha$  in membrane-initiated signaling in neural cells: Interaction with IGF-1  
701 receptor☆. *The Journal of Steroid Biochemistry and Molecular Biology* 114:2-7.
- 702 Meissirel C, Dehay C, Berland M, Kennedy H (1991) Segregation of callosal and association  
703 pathways during development in the visual cortex of the primate. *J Neurosci* 11:3297-  
704 3316.
- 705 Mitchell BD, Macklis JD (2005) Large-scale maintenance of dual projections by callosal and  
706 frontal cortical projection neurons in adult mice. *J Comp Neurol* 482:17-32.
- 707 Molyneaux BJ, Arlotta P, Hirata T, Hibi M, Macklis JD (2005) Fezl is required for the birth and  
708 specification of corticospinal motor neurons. *Neuron* 47:817-831.
- 709 Molyneaux BJ, Arlotta P, Fame RM, MacDonald JL, MacQuarrie KL, Macklis JD (2009) Novel  
710 Subtype-specific Genes Identify Distinct Subpopulations of Callosal Projection Neurons.  
711 *J Neurosci* 29.
- 712 Newbury DF, Bonora E, Lamb JA, Fisher SE, Lai CS, Baird G, Jannoun L, Slonims V, Stott  
713 CM, Merricks MJ, Bolton PF, Bailey AJ, Monaco AP, International Molecular Genetic  
714 Study of Autism C (2002) FOXP2 is not a major susceptibility gene for autism or specific  
715 language impairment. *Am J Hum Genet* 70:1318-1327.
- 716 Otsuka T, Kawaguchi Y (2011) Cell diversity and connection specificity between callosal  
717 projection neurons in the frontal cortex. *J Neurosci* 31:3862-3870.
- 718 Ozdinler PH, Macklis JD (2006) IGF-I specifically enhances axon outgrowth of corticospinal  
719 motor neurons. *Nat Neurosci* 9:1371-1381.

- 720 Polleux F, Dehay C, Goffinet A, Kennedy H (2001) Pre- and post-mitotic events contribute to
- 721 the progressive acquisition of area-specific connectional fate in the neocortex. *Cereb*
- 722 *Cortex* 11:1027-1039.
- 723 Razani B, Engelman JA, Wang XB, Schubert W, Zhang XL, Marks CB, Macaluso F, Russell
- 724 RG, Li M, Pestell RG, Di Vizio D, Hou H, Kneitz B, Lagaud G, Christ GJ, Edelmann W,
- 725 Lisanti MP (2001) Caveolin-1 null mice are viable but show evidence of
- 726 hyperproliferative and vascular abnormalities. *J Biol Chem* 276:38121-38138.
- 727 Rodriguez-Tornos FM, Briz CG, Weiss LA, Sebastian-Serrano A, Ares S, Navarrete M, Frangeul
- 728 L, Galazo M, Jabaudon D, Esteban JA, Nieto M (2016) Cux1 Enables Interhemispheric
- 729 Connections of Layer II/III Neurons by Regulating Kv1-Dependent Firing. *Neuron*
- 730 89:494-506.
- 731 Saito T (2006) In vivo electroporation in the embryonic mouse central nervous system. *Nat*
- 732 *Protoc* 1:1552-1558.
- 733 Saito T, Nakatsuji N (2001) Efficient gene transfer into the embryonic mouse brain using in vivo
- 734 electroporation. *Dev Biol* 240:237-246.
- 735 Schubert W, Frank PG, Woodman SE, Hyogo H, Cohen DE, Chow C-W, Lisanti MP (2002)
- 736 Microvascular hyperpermeability in caveolin-1 (-/-) knock-out mice. Treatment with a
- 737 specific nitric-oxide synthase inhibitor, L-NAME, restores normal microvascular
- 738 permeability in Cav-1 null mice. *J Biol Chem* 277:40091-40098.
- 739 Schwartz ML, Goldman-Rakic PS (1982) Single cortical neurones have axon collaterals to
- 740 ipsilateral and contralateral cortex in fetal and adult primates. *Nature* 299:154-155.

- 741 Schwartz ML, Goldman-Rakic PS (1984) Callosal and intrahemispheric connectivity of the  
 742 prefrontal association cortex in rhesus monkey: relation between intraparietal and  
 743 principal sulcal cortex. *J Comp Neurol* 226:403-420.
- 744 Silver J, Lorenz SE, Wahlsten D, Coughlin J (1982) Axonal guidance during development of the  
 745 great cerebral commissures: descriptive and experimental studies, in vivo, on the role of  
 746 preformed glial pathways. *J Comp Neurol* 210:10-29.
- 747 Sohur US, Padmanabhan HK, Kotchetkov IS, Menezes JR, Macklis JD (2014) Anatomic and  
 748 molecular development of corticostriatal projection neurons in mice. *Cereb Cortex*  
 749 24:293-303.
- 750 Takayasu Y, Takeuchi K, Kumari R, Bennett MV, Zukin RS, Francesconi A (2010) Caveolin-1  
 751 knockout mice exhibit impaired induction of mGluR-dependent long-term depression at  
 752 CA3-CA1 synapses. *Proc Natl Acad Sci U S A* 107:21778-21783.
- 753 Trushina E, Ducharme J, Parisi J, McMurray C (2006) Neurological abnormalities in caveolin-1  
 754 knock out mice. *Behav Brain Res* 172:24-32.
- 755 Vega CJ, Peterson DA (2005) Stem cell proliferative history in tissue revealed by temporal  
 756 halogenated thymidine analog discrimination. *Nat Methods* 2:167-169.
- 757 Wahlsten D, Metten P, Crabbe JC (2003) Survey of 21 inbred mouse strains in two laboratories  
 758 reveals that BTBR T/+ tf/tf has severely reduced hippocampal commissure and absent  
 759 corpus callosum. *Brain Res* 971:47-54.
- 760 Wang C, Zhang L, Zhou Y, Zhou J, Yang X, Duan S, Xiong Z, Ding Y (2007) Activity-  
 761 Dependent Development of Callosal Projections in the Somatosensory Cortex. *Journal of*  
 762 *Neuroscience* 27:11334-11342.

763 Woodworth MB, Greig LC, Liu KX, Ippolito GC, Tucker HO, Macklis JD (2016) Ctip1  
764 Regulates the Balance between Specification of Distinct Projection Neuron Subtypes in  
765 Deep Cortical Layers. Cell Rep 15:999-1012.

766 Zhao YL, Song JN, Zhang M (2014) Role of caveolin-1 in the biology of the blood-brain barrier.  
767 Rev Neurosci 25:247-254.

768

769

770

771

772

773

774

775

776

777

778

779

780

781 **Figure Legends**

782 **Figure 1: Caveolin1 is expressed by CPN and excluded from SCPN at postnatal day 3**

783 **(A-B)** Retrograde labeling was performed at postnatal day (P1) 1 by injecting CTB-647 into the  
784 contralateral hemisphere to label callosal projection neurons (A; CPN), and CTB-555 into the  
785 pons to label subcerebral projection neurons (B; SCPN). Example images of retrogradely-labeled  
786 brains are shown at P3, including wholemount images of the injection sites (dorsal view for  
787 CPN, ventral view for SCPN) and coronal sections showing the laminar distribution of the  
788 labeled neurons. **(C-C')** CAV1 (green) immunocytochemistry at P3 reveals that CAV1 is  
789 expressed in layer V, with a caudo-lateral distribution similar to SCPN (red). However, CAV1  
790 (green) colocalizes with retrogradely labeled CPN (blue) in layer Va, and it is excluded from  
791 SCPN (red) in layer Vb. The box in C indicates the region of higher magnification images in C'.  
792 **(D)** CAV1 expression (green) overlaps with the CPN developmental control SATB2 (red),  
793 reinforcing that CAV1 is expressed by CPN. **(E-F)** CAV1 expression is not altered in *Fezf2* null  
794 cortex (F), which is developmentally devoid of SCPN, reinforcing that CAV1 is not expressed by  
795 SCPN. Scale bars: (C) 250  $\mu$ m, (C') 100 $\mu$ m, (D) 250  $\mu$ m, (E,F) 500 $\mu$ m; P, postnatal day; IC,  
796 internal capsule; Th, thalamus; OB, olfactory bulb; Po, pons; Crb, cerebellum; roman numerals  
797 indicate cortical layer.

800 **Figure 2: Caveolin1 is expressed in caudo-lateral cortex during mid-stage cortical**  
801 **development.**

802 **(A)** *Cav1* mRNA is not detected in pallial progenitors or cortical plate at E13.5, but is  
803 detected in the caudal cortical hem. By E15.5, *Cav1* is expressed in the caudo-lateral

804 **cortical plate. (B) To determine whether *Cav1* expression follows a developmental gradient,**  
805 **we examined expression at later embryonic stages through postnatal development. *Cav1***  
806 **mRNA is expressed by a restricted population of layer Va cells (presumptive CPN) in the caudo-**  
807 **lateral cortex from late embryonic stages (E18.5) through early postnatal development (P3, P6),**  
808 **with expression reduced in the cortex by P14. (C) CAV1 protein is detected in a similar pattern**  
809 **to *Cav1* mRNA throughout development. CAV1 is expressed by CPN within the same caudo-**  
810 **lateral layer Va region throughout late embryonic and early postnatal development, suggesting**  
811 **that it is not following a developmental gradient. Scale bar: 1mm; E embryonic day; P, postnatal**  
812 **day.**

813

814

815 **Figure 3 CAV1 is expressed by layer Va CPN in an areally restricted fashion**

816 **(A-A')** Expression of CAV1 is areally restricted; CAV1 (green) is highly expressed by CPN  
817 **(red; CTB-555 retrograde label) throughout primary and secondary somatosensory cortex (S1**  
818 **and S2). CAV1 expression is not readily detected in CPN within motor cortex (M1), as**  
819 **delineated by layer II/III expression of LMO4 (blue). A', inset from A. Dashed line indicates M1**  
820 **– S1 boundary and cortical lamina. (B) In S1, CAV1 (green) is largely excluded from the CTIP2**  
821 **(red) expression domain (arrowheads) indicating SCPN, with only a small subpopulation of**  
822 **CTIP2+ve neurons extending into the CAV1 expression domain (arrow). (C) In S2, the boundary**  
823 **between CAV1 (green) and CTIP2 (red) is not as clearly defined, with more CTIP2+ve neurons**  
824 **interspersed with CAV1 (arrows). Regions of higher magnification insets are indicated in B' and**  
825 **C ". (D) At P6, *Cav1* is expressed in layer V, within the *Satb2* and *Bhlhb5*-expressing domain,**  
826 **and below the serotonin-expressing barrel cortex in layer IV. Regions of higher magnification**

insets are indicated in D' and D''. (E) CAV1-expressing neurons are born between days E12.5  
 and E13.5 in both S1 and S2. deoxyuridine analogs (CldU or IdU) were injected at 12 hour  
 intervals throughout corticogenesis, and immunocytochemistry for BrdU (red) and CAV1  
 (green) was performed at P3, revealing that CAV1-expressing neocortical neurons, both in  
 S1(somatosensory layer V) and S2 (caudolateral expansion) are born between E12.3 and E13.5.  
 (A') 500  $\mu$ m, (B-E) 100 $\mu$ m.

**Figure 4: CAV1 is expressed by restricted subpopulations of neocortical neurons at P8,**  
**predominantly dual projecting CPN/FPN**

Schematic representation of diverse populations of neocortical projection neurons with CPN  
 projecting subsets, including CPN (green), CPN with a dual ipsilateral forward projection  
 (CPN/FPN; red), CPN with a dual ipsilateral backward projection (CPN/BPN; magenta),  
 intratelencephalic corticostriatal projection neurons (CStrPNI; blue), and anterior commissure  
 projection neurons (ACN; yellow). (A-D) Retrograde labeling was performed for CPN (A;  
 green), FPN (B; red), BPN (C; red), and CStrPNI/ ACN (D; red). Both CPN and FPN are located  
 entirely within the CAV1 expression domain, as are a subset of the mixed population of CStrPNI  
 and ACN laterally (in S2). BPN are restricted to the rostro-medial cortex, outside the CAV1  
 expression domain. (E) To identify dual-projecting CPN/FPN, we simultaneously injected CTB-  
 647 into the ipsilateral premotor cortex and CTB-555 into the contralateral somatosensory  
 cortex, as indicated by the schematic in (E) and wholemount image in (E'). (E'') FPN are  
 isolated predominantly in layer V, with some in VIb (subplate) in largely lateral cortical  
 locations, with caudo-lateral S2 expansion. CPN are located in layers II/III, V, and VI. Dual  
 projecting CPN/FPN are located in layer Va in caudo-lateral cortex. (F) CAV1 is expressed by

851 over 80% of dual projecting CPN/FPN. Dual projecting CPN/FPN were labeled as shown in (E),  
852 and the percentage of dual projecting CPN/FPN that express CAV1 was calculated for four  
853 medio-lateral regions, listed +/- standard error of the mean (N = 4 brains). Scale bars: (A, B, C,  
854 D) 500  $\mu$ m, (A'-D', A''-D'') 100  $\mu$ m, (E'') 1mm; (F) 1mm, (F inset) 100  $\mu$ m.

855

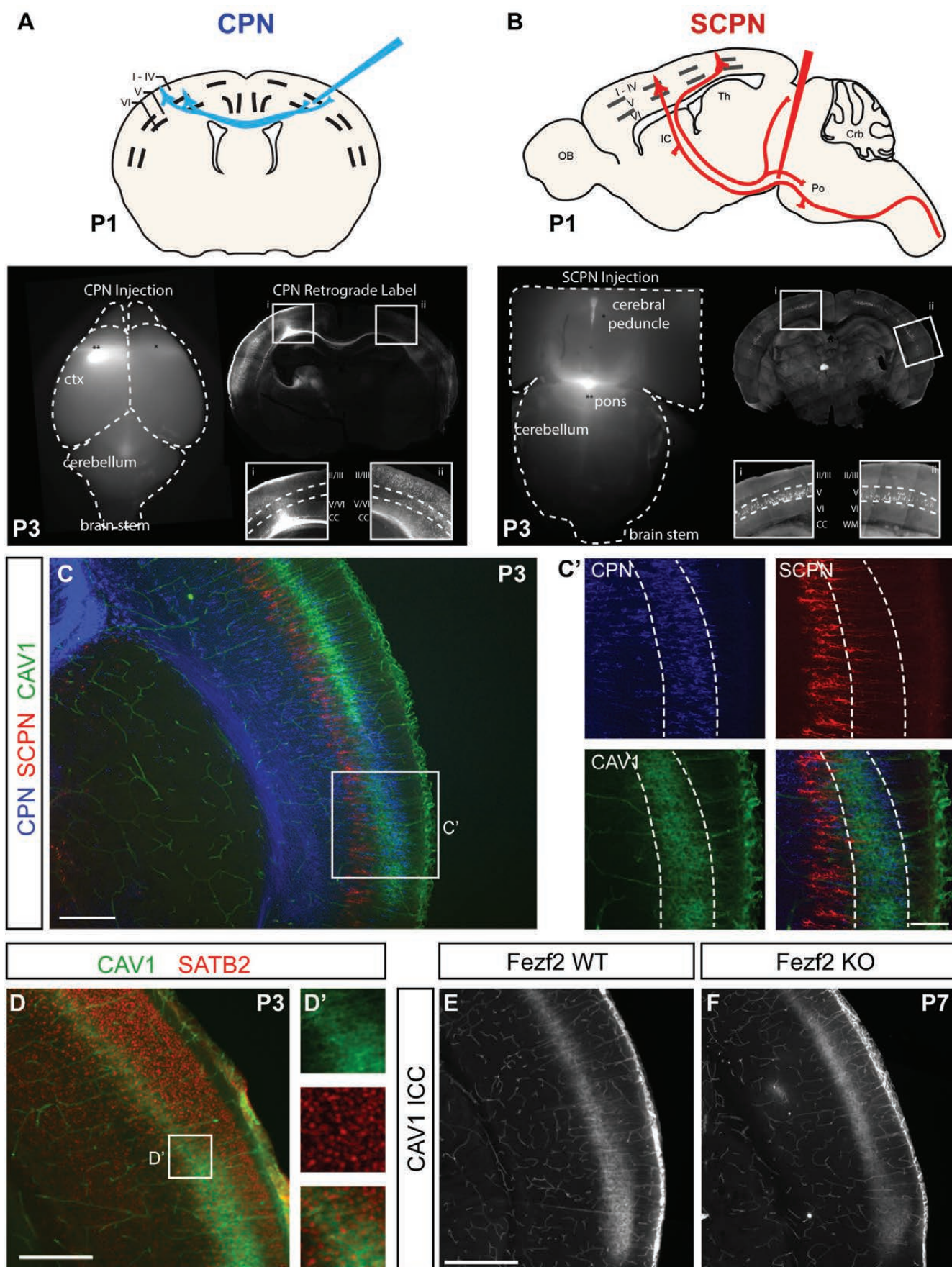
856 **Figure 5: CAV1 is localized to neuronal cell bodies and dendrites at postnatal ages**

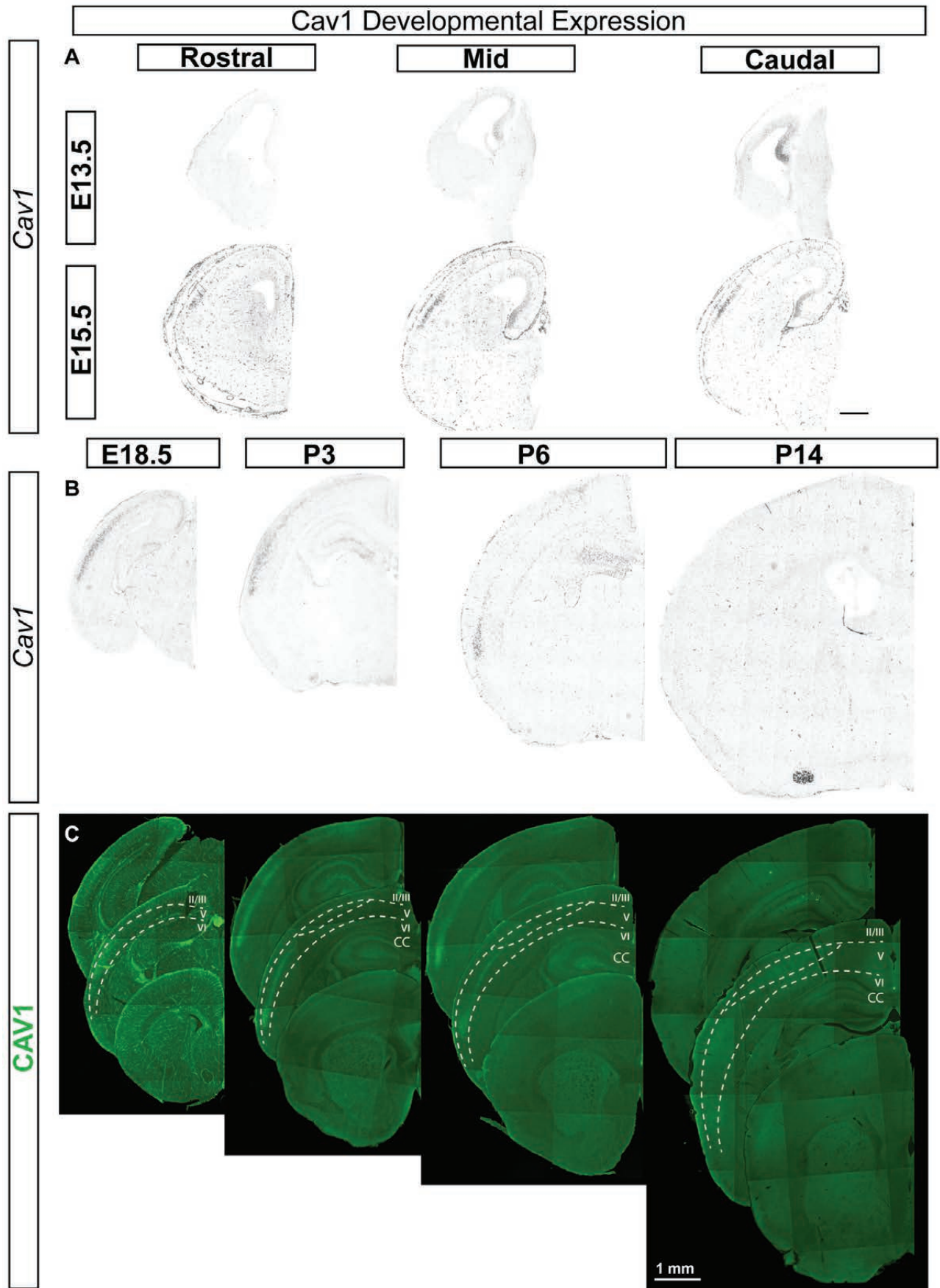
857 (A) CAV1 is detected within distinct layer Va neuronal cell bodies in S1 (arrowheads in A'),  
858 extending throughout their apical dendrites (asterisks in A'') and their dendritic arborizations at  
859 the pial surface (arrows in A''). (B-C) Exogenously expressing *Cav1* in superficial layer neurons  
860 of S1 by *in utero* electroporation at E15.5 does not disrupt migration or laminar location  
861 compared to a GFP-only control (C). (B'-C') Exogenous over-expression of *Cav1* results in  
862 CAV1 (red) protein localization that is similar to that of the endogenous protein (A), with CAV1  
863 localized to the cell bodies and dendritic compartments of the neuronal plasma membrane of  
864 superficial layer neurons at P6. Unlike GFP (green), CAV1 is not detected throughout the soma  
865 and nucleus, or distributed throughout neuronal processes (dendrites and axons). (B'') Higher  
866 magnification of B', comparing expression of CAV1 and GFP in soma (arrowheads), apical  
867 dendrites (asterisks), and dendritic tufts (arrows). (D) Correct CAV1 (green) expression is not  
868 dependent on formation of the corpus callosum at P4. Acallosal BTBR mice express CAV1 at  
869 comparable levels, and in an indistinguishable pattern, to their closely related callosal LPJ strain,  
870 indicating that CAV1 expression is not dependent on correct CPN connectivity. Scale bar: (A-  
871 A'') 20  $\mu$ m, (B,C) 250  $\mu$ m, (B',C') 50  $\mu$ m (D) 1mm.

872

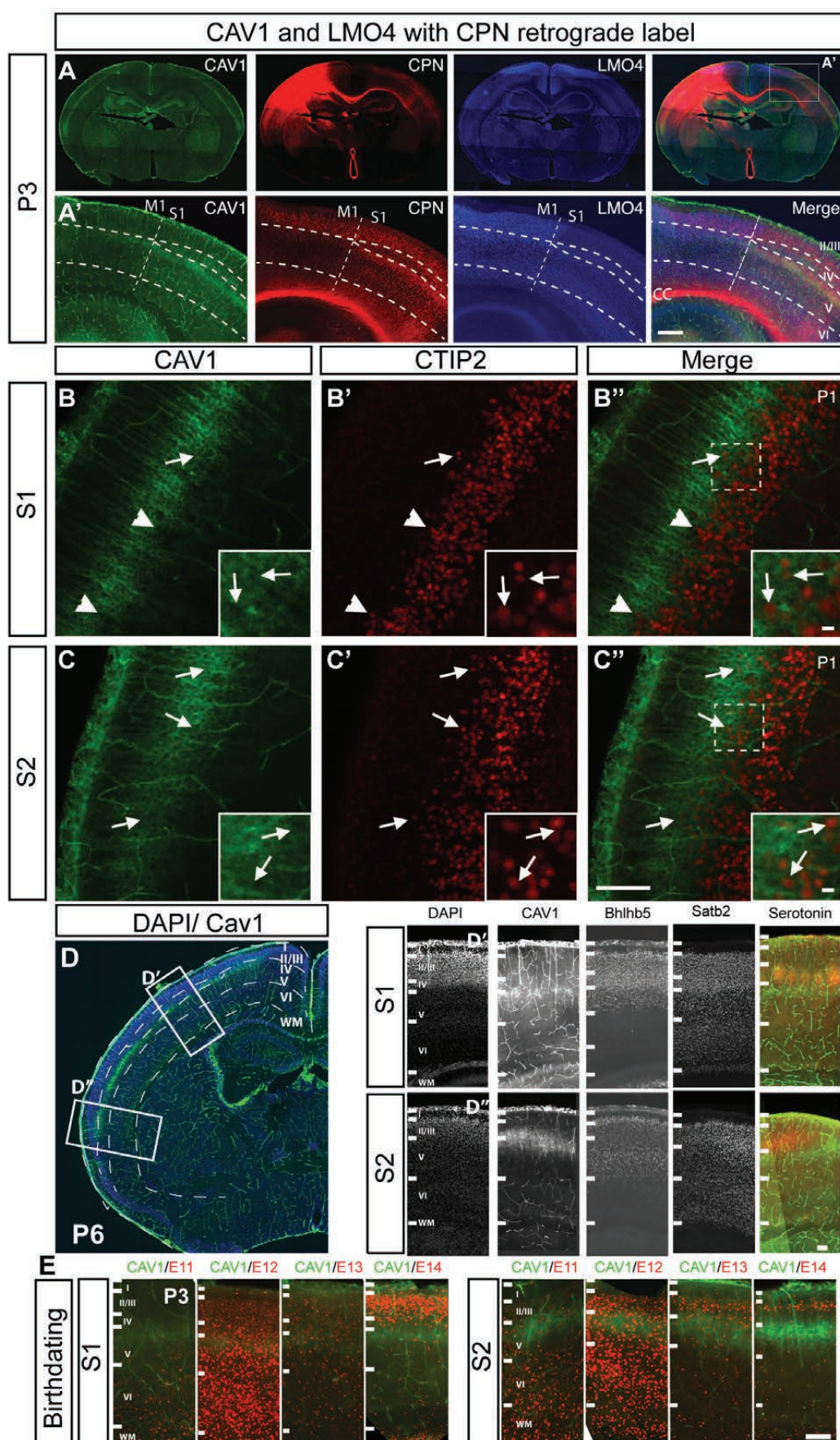


873 **Figure 6: Loss of *Cav1* function does not disrupt formation of dual projecting CPN/FPN**  
874 **axonal projections at P8.**  
875 (A-F) CPN (green) were retrogradely labeled from contralateral somatosensory cortex, and FPN  
876 (red) from ipsilateral premotor cortex in *Cav1* null mice (D-F; N = 5) and WT littermates (A-C;  
877 N = 5). (A, D) CPN, (B, E) FPN, and (C,F) CPN/FPN form in the absence of *Cav1* function. (G-  
878 H) The number of dual projecting CPN/FPN (G) and total FPN (H) were counted for 2 medio-  
879 lateral regions (S1 and S2). There is no significant difference between the two genotypes (N = 5  
880 WT and N = 5 *Cav1* nulls). (I) The percentage of total labeled FPN that have a dual callosal  
881 projection was also calculated for 2 medio-lateral regions (S1 and S2). There is no significant  
882 difference between the two genotypes (N = 5 WT and 5 *Cav1* null). Error bars denote standard  
883 error of the mean. CPN, callosal projection neurons; FPN, ipsilateral frontal projection neurons;  
884 WT, wildtype; P, postnatal day. Scale bars: (A-F) 500µm, (A'-F', A''-F'') 100µm.



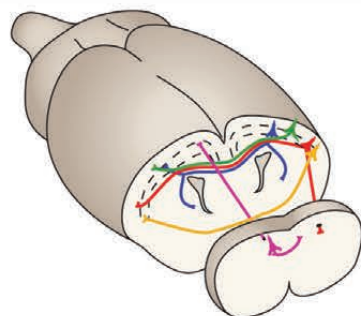






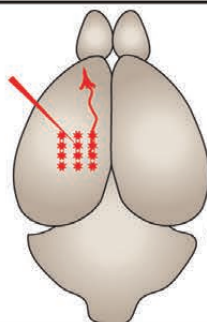


# Intracortical Projection Neuron Subtypes



CPN  
CPN/FPN  
CPN/BPN  
CStrPNi  
ACN

## BPN retrograde label



## CStrPN / AC retrograde label

